



Synthesis and antiproliferative studies of curcumin pyrazole derivatives

Honnalagere Ramesh Puneeth¹ · Hanumappa Ananda² ·
Kothanahally S. Sharath Kumar² · Kanchugarakoppal S. Rangappa² ·
Angatahally Chandrashekariah Sharada¹

Received: 25 January 2015 / Accepted: 27 June 2016
© Springer Science+Business Media New York

Abstract A series of curcumin pyrazole derivatives (**3a–e**) were synthesized. The chemical structures were determined by ¹H and ¹³C NMR spectroscopic techniques and their purity was confirmed by LC–MS and melting point determination. The compounds were screened for anticancer effects on different cancer cell lines by MTT (3-(4,5-Dimethylthiazol-2-yl)-2,5-Diphenyltetrazolium Bromide) assay. The analogs demonstrated growth inhibitory effect on MCF-7, HeLa, and K562 cell lines with significant IC₅₀ values. Compound **3b** exhibited a high degree of cytotoxicity against cancer cells and minimum growth inhibitory effects against normal cells HEK293T and hence further, cell cycle analysis and mitochondrial membrane potential studies (JC-1 assay) were conducted by utilizing flow cytometry against K562 cells. This compound effectively arrested cell cycle progression at SubG1 phase and cells exhibited decreased membrane potential in a concentration-dependent manner with fluorescence shifting from red to green. Our findings suggest that compound **3b** could be a promising anticancer agent since it effectively inhibited cell proliferation and can be selected for further in vitro and in vivo investigations.

Keywords Leukemic cells · Cytotoxicity · Anticancer · Cell cycle

Introduction

The fight against cancer is a global effort. Despite of significant advances in diagnosis and treatment, cancer is still a life threatening disease around the world. Recent investigations have focused on naturally occurring chemopreventive compounds possessing anticancer potential with minimal toxicity. Most of the anticancer drugs approved during 1981–2002 are natural products and their derivatives (Newman et al., 2003).

Curcumin is a polyphenol compound obtained from the rhizome (turmeric) of the plant *Curcuma longa* and is the major active constituent in turmeric. Pharmacologically, curcumin has been found to be safe even at very high doses in human clinical trials (Aggarwal et al., 2003). It has been widely used for various ailments due to its medicinal properties (Aggarwal et al., 2007). The anticancer potential of curcumin has been demonstrated in various cell lines (Aggarwal et al., 2006; Senft et al., 2010) and can induce apoptosis in a variety of cell lines including GBC-SD, HT-29, JURKAT, H520 (Liu et al., 2013; Wang et al., 2013; Gopal et al., 2014).

However, curcumin is not regarded as a potent therapeutic molecule as potential utility of curcumin is restricted because of its in vivo bioavailability. Curcumin decomposes rapidly in neutral and basic conditions. In addition, curcumin extensively undergoes in vitro and in vivo Phase I and Phase II metabolism (Wang et al., 1997; Pan et al., 1999; Anand et al., 2007).

Multiple approaches are being hunted to overcome these limitations. Synthetic chemical modifications of curcumin

Electronic supplementary material The online version of this article (doi:10.1007/s00044-016-1628-5) contains supplementary material, which is available to authorized users.

✉ Angatahally Chandrashekariah Sharada
sharadaac@gmail.com

¹ Department of Biochemistry, Yuvaraja's College, University of Mysore, Mysuru 570005 Karnataka, India

² Department of Studies in Chemistry, Manasagangotri, University of Mysore, Mysuru 570006 Karnataka, India

structure have been studied and various curcumin analogs are synthesized to improve the therapeutic profile of the natural product. New analogs of curcumin exhibited antiangiogenic, antitumor, and growth suppressive activities 30 times than natural curcumin (Chandru and Sharada, 2007; Davis et al., 2008; Youssef et al., 2005; Ohori et al., 2006) and an analog of curcumin showed potent growth inhibitory activities on both prostate and breast cancer cell lines and was 50 times more potent than curcumin (Fuchs et al., 2009). In this context, we synthesized ethanone pyridine curcumin analogs and cyclopropoxy curcumin analogs which exhibited in vivo growth inhibitory and antiangiogenic effects against a mouse tumor model (Chandru and Sharada, 2007; Chandru et al., 2007, 2008) in our previous investigations.

In this line of continuation, in the present study, we have synthesized and investigated the antiproliferative potential of curcumin pyrazole derivatives against various cancer cell lines.

Results

Chemistry

Curcumin analogs (**3a–3e**) was synthesized by base catalyzed cyclization of different phenyl hydrazines with curcumin in the presence of ethanol under reflux condition (Fig. 1). Both electron-donating substituent and electron withdrawing substituent on phenyl hydrazines underwent cyclization smoothly with curcumin to produce pyrazole derivatives (Mayadevi et al., 2012; Kumar et al., 2012; Pramod et al., 2012; Mishra et al., 2008). Proton and carbon NMR spectral data are convinced with the proposed structure and physicochemical data of all the compounds are listed in Table 1.

Bioavailability studies

ADME (absorption, distribution, metabolism, and excretion) properties were calculated in Qikprop simulation. All the

compounds obey the Lipinski's rules within four violation; molecular weight below 500 Da, hydrogen bond donor (<5) and acceptor (<10). QPlogPo/w (octanol/water partition coefficient) for all the compounds is <5. Total solvent accessible surface area (SASA), hydrophobic component of the SASA (FOSA), and hydrophilic component of the SASA (FISA) were analyzed for the compounds that were abiding the ranges in Qikprop physicochemical properties (Data not shown). Qualitative model for human oral absorption was predicted, Curcumin showed high oral absorption comparatively against **3a**, **3c**, **3d**, and **3e** which showed low, and **3b** showed medium oral absorption (Table 2). Polar nitrogen and oxygen, and Van der Waals surface area (PSA) of compounds were fulfilling the limit in physicochemical calculation. All the ligands satisfy the values of partition coefficient of octanol/gas (QPlogPoc), water/gas (QPlogPw) and brain/blood (QPlogBB), skin permeability (QPlogKp), aqueous solubility (QPlogS), and predicted for compounds lie in the allowed solubility and permeability range (Data not shown) (Fig. 2)

Molecule docking has been successfully carried out to design novel potential leads. A total of five validated potential leads are suggested from the study among which **3b** satisfy ADME drug criteria. ADME result suggest that the oral administration potency might be medium in case of **3b**, but its availability to get into moderate when compared to range of 95 % standard drugs. Thus it validates that **3b** could be a potential cytotoxic agent.

Biological activities

Cell growth suppression analysis by MTT assay

All compounds were evaluated for in vitro cytotoxicity against three cancer cell lines, MCF-7, HeLa, and K562 cells by MTT assay. Paclitaxel drug was used as positive control and curcumin was taken as a standard reference. The results of cytotoxicity studies of curcumin analogs (**3a–3e**) were recorded at different doses and at different time intervals, and are presented as IC₅₀ values, the mean

Fig. 1 Synthesis of pyrazole analogs of curcumin

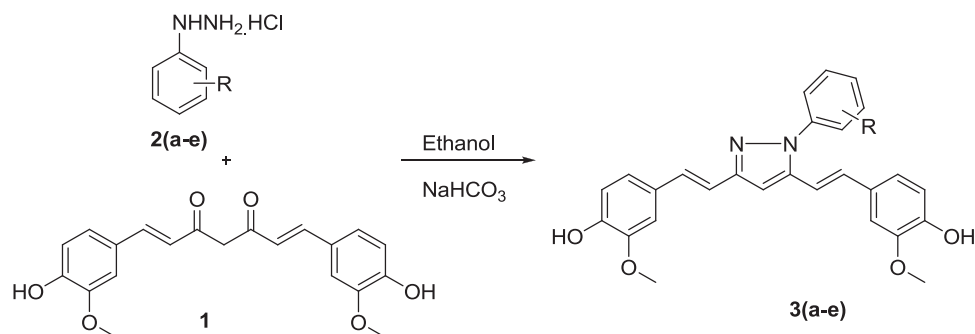
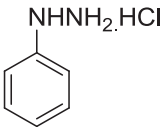
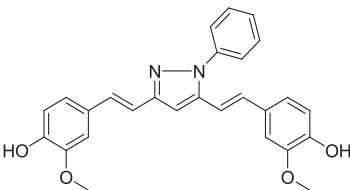
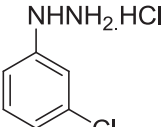
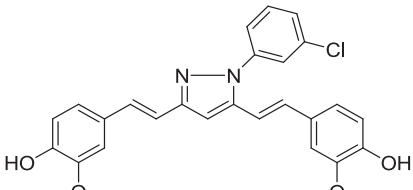
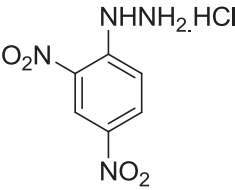
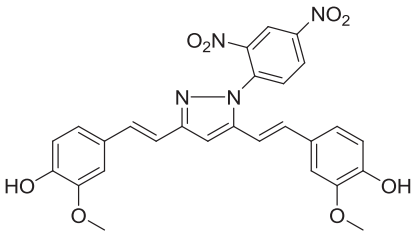
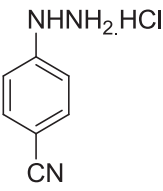
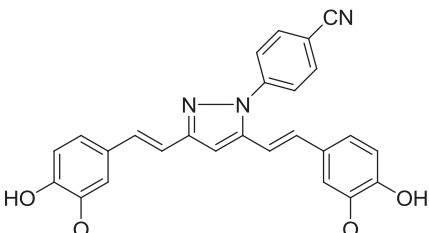
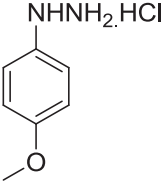
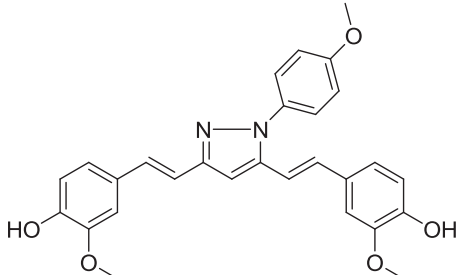


Table 1 Curcumin pyrazole analogs, synthesis of curcumin pyrazole derivatives

Entry ^a	2	3	Time (h)	Yield ^{b,c} (%)
1			13	91 (Mayadevi et al., 2012)
2			14	89 (Kumar et al., 2012)
3			15	75 (Pramod et al., 2012)
4			14	86
5			12	92 (Mishra et al., 2008)

^a Curcumin (1 equivalent), phenyl hydrazines (1.5 equivalent) and NaHCO₃ (1.5 equivalent)^b Isolated yield^c Literature reported compound

growth inhibitory concentration and are summarized in Table 3.

The data obtained by MTT assay showed that compound **3a**, **3b**, and **3c** have considerable inhibitory effects on the growth of cancer cell lines after 48 and 72 h of treatment. Compound **3b** was found to be more effective and showed

significant growth inhibitory effects against all the three cancer cell lines. Compound **3b** was tested for cytotoxicity against HEK293T cells and was found to be nontoxic. Among the cancer cells tested, K562 cells were more sensitive to this compound and were selected for further studies.

Table 2 ADME (Adsorption digestion metabolism and excretion) result of the compounds used for insilico molecular docking

Predictions for properties	ADME result					(Range 95 % of drugs)
	Curcumin	3a	3b	3c	3d	3e
log K hsa serum protein binding	-0.027	1.17	1.28	0.76	1.01	1.18
log BB for brain/blood	-1.827	-0.97	-0.82	-2.7	-1.91	-1.05
HERG K+Channel Blockage: log IC50	-6.418	-7.77	-7.6	-7.46	-7.81	-7.61
QP log P for octanol/water	3.039	6.3	6.5	4.60	5.58	6.42
Predicted apparent Caco-2 cell permeability in nm/s	345	1656	1660	75	343	1655
Predicted apparent MDCK cell permeability in nm/s (MDCK cells are considered to be a good mimic for the blood-brain barrier)	156M	853M	1959M	30M	155M	853M
QP log Kp for skin permeability	-2.174	-0.28	-0.44	-3.02	-1.63	-0.38
Percentage of human oral absorption in GI (± 20 %)	90	100	100	88	92	100
Qualitative, model for human oral absorption	High	Low	Medium	Low	Low	Low
Lipinski rule of 5 violations	0	1	1	0	1	1
						Maximum is 4

The effect of curcumin analog **3b** on cell cycle progression

After preliminary investigations of MTT assay, the effect of compound **3b** on cell cycle progression was examined by fluorescence activated cell sorter. The concentrations were selected based on growth inhibitory studies. K562 cells were processed, stained with propidium iodide, and subjected to flow cytometric analysis. The histogram of control cells (DMSO-treated) showed a standard pattern of cell cycle progression. Cell population in different cell cycle phases of control was found to be 38.86, 30.64, 13.38, and 8.89 % in G1, S, SubG1, and G2 phases respectively. Cell cycle progression was altered upon addition of the compound **3b**. The 10 and 20 μ M concentrations of compound **3b** did not induce a significant effect on cell cycle progression. The cell distribution pattern in 40 μ M, compound **3b** treated K562 cells was found to be 8.89, 13.15, 23.53, and 39.64 % in G1, S, SubG1, and G2 phases, respectively. In this concentration at 40 μ M, compound **3b** treated cells were significantly arrested in the SubG1 phase showing accumulation of cells.

JC-1 assay to detect changes in mitochondrial membrane potential by flow cytometry

The cell death induced by compound **3b** in K562 cells was analyzed by JC-1 staining assay by flow cytometric analysis. Changes in the mitochondrial membrane potential were determined by red vs. green fluorescence where healthy mitochondria gives out red fluorescence and apoptotic/dead cells emits green fluorescence because of lack of mitochondrial membrane potential. Cells exposed to the 2, 4-DNP was used as positive control and DMSO-treated cells served as a vehicle control. Minimum 10,000 events were acquired and analyzed by using CellQuest Pro software (BD, USA). Panels representing flow cytometric density plots were used to determine the results, which are depicted in Fig. 3. DMSO-treated cells showed 26.5 % of green fluorescence whereas 2, 4-DNP-treated cells showed 68.92 % of green fluorescence. Compound **3b** exhibited 53.60, 86.62, and 93.30 % of green fluorescence at 10, 20, and 40 μ M, respectively. Results revealed that compound **3b** induced a significant depolarization of mitochondrial membrane potential at 20 and 40 μ M that was indicated by shifting of fluorescence from red to green. The effect was increased linearly in a concentration-dependent manner in leukemic (K562) cells.

Discussion

Cancer treatment is one of the many focused areas of interest in the current research. Chemoprevention has evolved as a

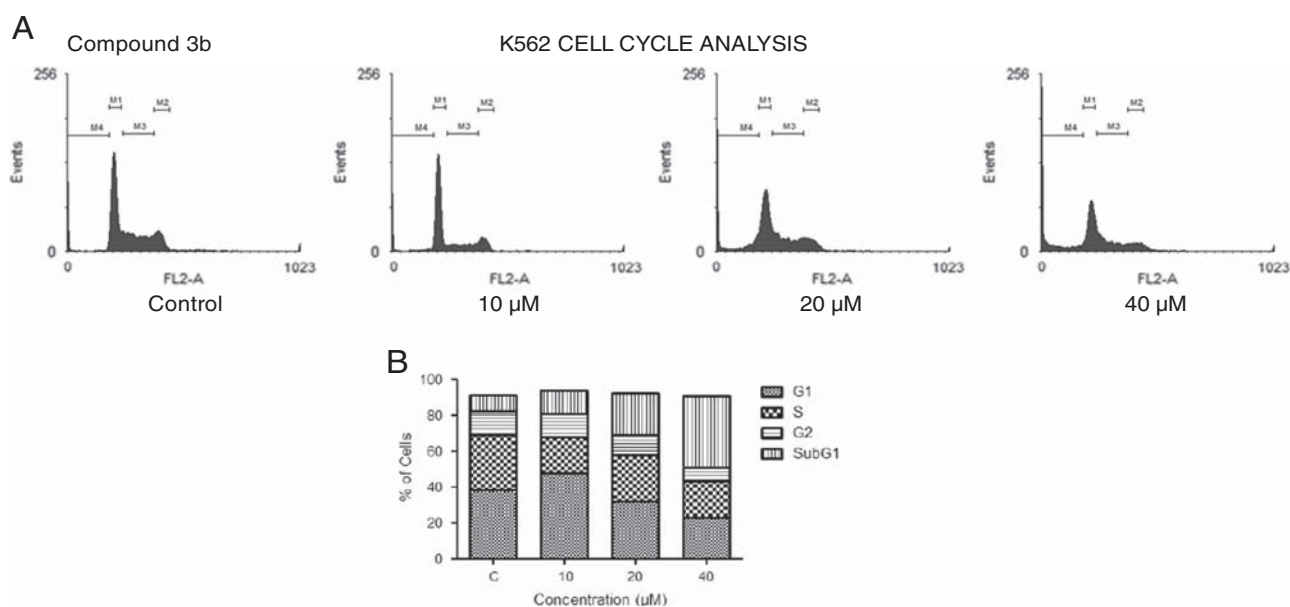


Fig. 2 Effect of curcumin analog **3b** (10, 20, and 40 μ M, respectively) on cell cycle progression in K562 cells. **a** Histogram obtained after FACS analysis for K562 cells. **b** Bar graph showing the percentage of

cells in the SubG1, G1, S, and G2 phases of the cell cycle. The data presented is derived from two independent experiments and error bars are indicated

Table 3 Effect of of curcumin analogs (**3a–3e**) against three human cancer cell lines in MTT assay expressed in IC_{50} values

Compounds	Cell lines (IC_{50} values in μ M)			
	HeLa	MCF-7	K562	HEK293T
Curcumin	46.60	37.84	28.86	NT
3a	42.54	52.88	36.99	NT
3b	45.56	34.99	25.55	>1000
3c	56.45	43.60	42.35	NT
3d	78.12	>100	85.21	NT
3e	83.12	81.88	75.12	NT
Paclitaxel	0.0061	0.0053	0.0049	NT

NT Not tested

finer strategy to control malignancy with minimum secondary effects than classical chemotherapy (Tsao et al., 2004; Steward & Brown, 2013). But, chemotherapeutic and chemopreventive drugs usually lack multiple targeting ability on cancer cells and are non-selective in their action and hence toxic to normal healthy cells with undesirable side effects. An ultimate drug should target cancer cells in multiple ways and should possess minimal toxicity against normal cells. Many natural products are screened for their antitumor potential from the past few decades in this aspect (Devi et al., 1999; Rocha et al., 2001; Yin et al., 2013). Curcumin, an active component of turmeric inhibits malignant cells through multiple pathways and also ensures cytoprotection selectively against normal cells due to its polyphenolic nature (Duvoix

et al., 2005; Thangapazham et al., 2006). Curcumin inhibits various cell cycle phases in different cell lines (Liu et al., 2007; Anand et al., 2008; Lee et al., 2009). Though curcumin fulfills the criteria of an ideal chemopreventive drug, various efforts have been undergone to overcome the limitations of curcumin and to improve its therapeutic efficacy. The development of chemical modifications in the structure of curcumin is one of the possible approaches to advance its anticancer efficiency (Anand et al., 2008; Fuchs et al., 2009). On the other hand, pyrazoles are the crucial bioactive moiety and received considerable attention in the pharmacological research with promising anticancer activities in various cancer models (Balbi et al., 2011; Koca et al., 2013; Shamroukh et al., 2014).

In this perspective, a series of curcumin pyrazole derivatives (**3a–3e**) were synthesized. These compounds were assessed for bioavailability and screened for anticancer activities. The efficiency of anticancer drugs can be assessed by their ability to suppress the proliferation of tumor cells. MTT assay is a reliable method to measure the proliferative rate and cell death (Ferrari et al., 1990). Cytotoxicity of curcumin pyrazoles (**3a–3e**) was investigated by using MTT assay on HeLa, MCF-7, and K562 cell lines. All the compounds in the series exhibited growth inhibitory effects on all the three cancer cell lines. Compound **3b** was found to be more potent and was more effective than curcumin in HeLa and K562 cell lines. Compound **3b** was also found to be nontoxic with negligible growth inhibitory effects against normal cells HEK293T.

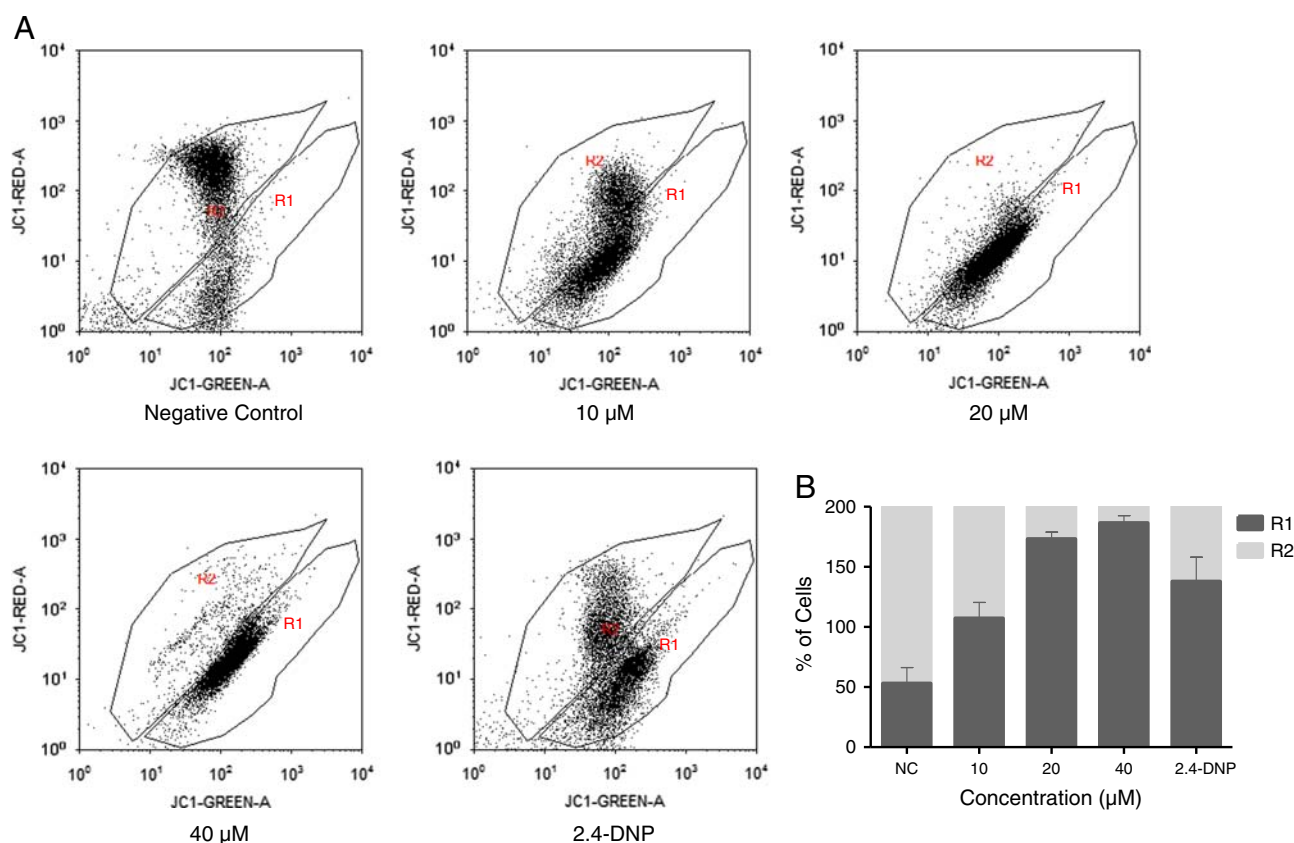


Fig. 3 Effect of curcumin analog **3b** (10, 20, and 40 μ M, respectively) on mitochondrial membrane potential by JC-1 staining assay. **a** Dot plot representing JC-1 stained K562 cells at various concentrations of

compound **3b**. **b** Bar graph showing percentage of red vs. green fluorescing cells, which represents high and low mitochondrial membrane potential. (R2 and R1 respectively)

K562 cells were more sensitive to compound **3b** treatment than other two cell lines screened and hence K562 cells were selected for further studies.

We utilized the flow cytometry to detect the cell cycle progression. DMSO-treated K562 cells (control) underwent a normal cell cycle with high amount of cell populations in G1 phase whereas cells accumulated significantly at SubG1 phase (39.64 %) after treatment with compound **3b** at 40 μ M concentration for 48 h. Accumulation of cells in the SubG1 phase is an early indicator of apoptosis (Fujii et al., 2013). Our findings suggest that compound **3b** induces cell death, which resulted in increased cell population in the SubG1 phase, which may lead to apoptosis, thereby affecting its proliferation and was further confirmed by mitochondrial membrane studies.

Anticancer compounds inducing apoptosis always show a rapid collapse in the mitochondrial membrane potential. Loss of mitochondrial membrane potential is one of the early events in apoptotic cascade and it can be detected by JC-1 staining, a sensitive assay (Ly et al., 2003). JC-1 is a cationic dye that can selectively enter into mitochondria where it aggregates and shows red fluorescence in normal cells. In apoptotic cells, the mitochondrial membrane

potential collapses resulting in distribution of JC-1 reagent throughout the cell in a monomeric state that fluoresces green color. We employed JC-1 staining assay to investigate the effect of compound **3b** on the mitochondrial membrane potential. The ratio of the red to green fluorescence in the compound treated with K562 cells significantly declined at 48 h compared to the control in a dose-dependent manner. Compound **3b** is capable of disrupting mitochondrial membrane potential significantly at low concentrations (10, 20, and 40 μ M) which was an indication of apoptosis.

From the studies we found that the compound **3b** treatment effectively inhibits the proliferation of K562 cells via an induction of apoptosis. However, further experiments need to be performed to investigate the specific markers of apoptotic cells and further mechanism of action of compound **3b** in future in vitro studies.

Conclusion

A series of curcumin pyrazole derivatives were synthesized and are evaluated for their cytotoxic potential. All the

curcumin pyrazole derivatives showed considerable growth inhibitory activities in all the cell lines (HeLa, MCF-7, and K562), whereas compound **3b** exhibited significant activity. The electron-donating capacity of chlorine atom could be the key aspect for the better activity than other substituents. Compound **3b** was found to be selectively nontoxic against normal cells and was more potent against cancer cells. Experimental studies against K562 cells revealed that compound **3b** induced cell death by SubG1 phase arrest in cell cycle and induced cell damage by causing depolarization of mitochondrial membrane potential. Thus from the findings we can conclude that, the synthetic analog of curcumin, compound **3b** [4,4'-(1*E*,1'*E*)-2,2'-(1-(3-chlorophenyl)-1*H*-pyrazole-3,5-diyl)bis(ethene-2,1-diyl)bis(2-methoxyphenol)] could be a promising, inexpensive anticancer drug effective at nontoxic doses. The structural modification of compound **3b** to improve its bioavailability without affecting its activity is underway in our laboratory.

Experimental

Chemistry

All the chemicals were supplied from Merck, Aldrich, and Fluka. The melting points were determined on capillary tubes on a Büchi oil heated melting point apparatus and are uncorrected. Reactions were monitored by TLC using pre-coated sheets of silica gel G/UV-254 of 0.25 mm thickness (Merck 60F254) using UV light for visualization. ^1H and ^{13}C NMR spectra were recorded on a NMR spectrometer operating at 400 and 100 MHz, respectively, using the residual solvent peaks as reference relative to SiMe_4 . Mass spectra were recorded using high resolution mass spectrometer. Infrared spectra were recorded on Shimadzu FT-IR model 8300 spectrophotometer.

General procedure for the synthesis of compounds (**3a–3e**)

To a solution of curcumin (1 equivalent) in ethanol, NaHCO_3 (1.5 equivalent), and different phenylhydrazine hydrochlorides (1.5 equivalent) were added. The resulting mixture was refluxed for 12–15 h and the reaction was monitored by TLC. After completion of the reaction, mixture was evaporated under reduced pressure and the resulting residue was dissolved with ethyl acetate and washed with water followed by the brine solution. The organic layer was dried over anhydrous sodium sulfate and evaporated under vacuum to get the crude product, which was purified by column chromatography using hexane: ethyl acetate as an eluent.

4,4'-(1*E*,1'*E*)-2,2'-(1-phenyl-1*H*-pyrazole-3,5-diyl)bis(ethene-2,1-diyl)bis(2-methoxyphenol) (**3a**) Pale brown solid (MeOH) compound (**3a**) was prepared from curcumin (**1**) (1.35 mmol, 0.50 g) and phenylhydrazine hydrochloride (**2a**) (2.03 mmol, 0.29 g) according to the general procedure. The product obtained as a pale brown solid was purified from methanol: 0.54 g (91 %); m.p. 89–91 °C (Mayadevi et al., 2012; 88–89 °C); ^1H NMR (400 MHz, DMSO- d_6): δ 3.75 (s, 3H, OCH_3), 3.81 (s, 3H, OCH_3), 6.72–6.76 (m, 3H), 6.90–7.04 (m, 5H), 7.11–7.19 (m, 3H), 7.41–7.45 (m, 1H), 7.49–7.56 (m, 4H, ArH), 9.12 (s, 1H, OH), 9.23 (s, 1H, OH); ^{13}C NMR (100 MHz, DMSO- d_6): δ 56.0 (OCH_3), 56.1 (OCH_3), 101.2 (ArC–H), 110.1 (2 \times ArC–H), 111.0 (Pyrazole C=C), 112.6 (ArC–H), 116.0 (2 \times ArC–H), 116.1 (C=C), 117.8 (ArC–H), 120.6 (ArC–H), 125.1 (C=C), 128.0 (ArC–H), 128.2 (ArC–H), 128.8 (ArC–H), 129.7 (2 \times Ar–C), 131.1 (C=C), 133.2 (C=C), 139.7 (ArC–N), 142.7 (Pyrazole C–N), 147.2 (ArC–OH), 147.8 (ArC–OH), 148.2 (ArC– OCH_3), 148.3 (ArC– OCH_3), 151.4 (Pyrazole C=N). LCMS (ESI) m/z $[\text{M} + 1]^+$ 441.51; Anal. calcd for $\text{C}_{27}\text{H}_{24}\text{N}_2\text{O}_4$: C, 73.62; H, 5.49; N, 6.36; O, 14.53 Found: C, 73.65; H, 5.52; N, 6.34; O, 14.55.

4,4'-(1*E*,1'*E*)-2,2'-(1-(3-chlorophenyl)-1*H*-pyrazole-3,5-diyl)bis(ethene-2,1-diyl)bis(2-methoxyphenol) (**3b**) Brown solid this (MeOH) compound (**3b**) was prepared from curcumin (**1**) (1.35 mmol, 0.50 g) and 3-chloro phenylhydrazine hydrochloride (**2b**) (2.03 mmol, 0.36 g) according to the general procedure. The product obtained as a brown solid was purified from methanol: 0.57 g (89 %); m.p. 116–118 °C; ^1H NMR (400 MHz, DMSO- d_6): δ 3.79 (s, 3H, OCH_3), 3.84 (s, 3H, OCH_3), 6.78–6.85 (m, 3H), 6.96–7.22 (m, 8H), 7.51–7.64 (m, 4H, ArH), 9.17 (s, 1H, OH), 9.29 (s, 1H, OH). ^{13}C NMR (100 MHz, DMSO- d_6): δ 56.06 (OCH_3), 56.11 (OCH_3), 101.8 (ArC–H), 110.1 (ArC–H), 110.9 (Pyrazole C=C), 112.4 (ArC–H), 116.0 (ArC–H), 116.1 (C=C), 117.5 (ArC–H), 120.7 (ArC–H), 120.9 (ArC–H), 123.5 (ArC–H), 124.7 (C=C), 127.8 (ArC–H), 128.1 (Ar–C), 128.7 (Ar–C), 131.4 (C=C), 131.6 (ArC–H), 133.7 (C=C), 134.0 (ArC–Cl), 140.9 (Pyrazole C–N), 143.0 (ArC–N), 147.3 (ArC–OH), 147.9 (ArC–OH), 148.2 (ArC– OCH_3), 148.3 (ArC– OCH_3), 151.9 (Pyrazole C=N). LCMS (ESI) m/z $[\text{M} + 1]^+$ 475.97; Anal. calcd for $\text{C}_{27}\text{H}_{23}\text{ClN}_2\text{O}_4$: C, 68.28; H, 4.88; Cl, 7.46; N, 5.90; O, 13.48 Found: C, 68.32; H, 4.91; Cl, 7.49; N, 5.89; O, 13.51.

4,4'-(1*E*,1'*E*)-2,2'-(1-(2,4-dinitrophenyl)-1*H*-pyrazole-3,5-diyl)bis(ethene-2,1-diyl)bis(2-methoxyphenol) (**3c**) Red solid (MeOH) compound (**3c**) was prepared from curcumin (**1**) (1.35 mmol, 0.50 g) and 2,4-dinitro phenylhydrazine hydrochloride (**2c**) (2.03 mmol, 0.47 g) according to the general procedure. The product obtained as a red solid was purified from methanol. 0.54 g (75 %); m.p. 119–121 °C; (Pramod et al., 2012, 118–119 °C); ^1H NMR (400 MHz,

DMSO-d₆): δ 3.78 (s, 3H, OCH₃), 3.88 (s, 3H, OCH₃), 6.65–6.82 (m, 4H), 6.91–7.48 (m, 10H). ¹³C NMR (100 MHz, DMSO-d₆): δ 56.2 (OCH₃), 56.4 (OCH₃), 109.1 (ArC–H), 109.3 (ArC–H), 110.3 (Pyrazole C=C), 116.1 (C=C), 116.5 (ArC–H), 116.7 (ArC–H), 120.4 (ArC–H), 122.7 (ArC–H), 122.9 (ArC–H), 123.3 (ArC–H), 124.1 (C=C), 127.9 (ArC–H), 130.1 (2× ArC–), 130.9 (C=C), 131.5 (C=C), 136.6 (Pyrazole C–N), 139.8 (ArC–N), 142.6 (ArC–NO₂), 146.5 (ArC–NO₂), 147.5 (ArC–OH), 147.8 (ArC–OH), 149.3 (ArC–OCH₃), 149.6 (ArC–OCH₃), 152.5 (Pyrazole C=N). LCMS (ESI) m/z [M + 1]⁺ 531.53; Anal. calcd for C₂₇H₂₂N₄O₈ : C, 61.13; H, 4.18; N, 10.56; O, 24.13 Found: C, 61.15; H, 4.21; N, 10.58; O, 24.12.

4-(3,5-bis(4-hydroxy-3-methoxystyryl)-1H-pyrazol-1-yl) benzonitrile (**3d**) Yellowish brown solid (MeOH) compound (**3d**) was prepared from curcumin (**1**) (1.35 mmol, 0.50 g) and 4-cyano phenylhydrazine hydrochloride (**2d**) (2.03 mmol, 0.34 g) according to the general procedure. The product obtained as a yellowish brown solid was purified from methanol: 0.54 g (86 %); m.p. 119–121 °C; ¹H NMR (400 MHz, DMSO-d₆): δ 3.80 (s, 3H, OCH₃), 3.85 (s, 3H, OCH₃), 6.79–6.91 (m, 3H), 6.99–7.23 (m, 8H), 7.75–7.77 (d, J = 8.4 Hz, 2H, ArH), 8.01–8.03 (d, J = 8.8 Hz, 2H, ArH). ¹³C NMR (100 MHz, DMSO-d₆): δ 56.0 (OCH₃), 56.1 (OCH₃), 102.7 (ArC–H), 109.8 (ArC–H), 110.1 (ArC–H), 111.1 (ArC–H), 112.4 (Pyrazole C=C), 116.0 (2× ArC–H), 116.1 (C=C), 117.3 (ArC–H), 118.9 (C≡N), 120.8 (ArC–H), 121.1 (ArC–H), 125.0 (C=C), 128.1 (ArC–), 128.6 (ArC–), 132.1 (C=C), 134.1 (C=C), 134.2 (2× ArC–H), 143.2 (Pyrazole C–N), 143.4 (ArC–N), 147.5 (2× ArC–OH), 148.0 (ArC–OCH₃), 148.3 (ArC–OCH₃), 152.6 (Pyrazole C=N). LCMS (ESI) m/z [M + 1]⁺ 466.52; Anal. calcd for C₂₈H₂₃N₃O₄ : C, 72.24; H, 4.98; N, 9.03; O, 13.75 Found: C, 72.27; H, 4.99; N, 9.06; O, 13.78.

4,4'-(1E,1'E)-2,2'-(1-(4-methoxyphenyl)-1H-pyrazole-3,5-diyl)bis(ethene-2,1-diyl)bis(2-methoxyphenol) (**3e**) Dark brown solid (MeOH) compound (**3e**) was prepared from curcumin (**1**) (1.35 mmol, 0.50 g) and 4-methoxy phenylhydrazine hydrochloride (**2d**) (2.03 mmol, 0.35 g) according to the general procedure. The product obtained as a dark brown solid and was purified from methanol: 0.58 g (92 %); m.p. 107–109 °C; (Mishra et al., 2008; 106 °C); ¹H NMR (400 MHz, DMSO-d₆): δ 3.90 (s, 6H, OCH₃), 3.91 (s, 3H, OCH₃), 6.80 (s, 1H), 6.98–7.02 (m, 4H), 7.08–7.19 (m, 6H), 7.29–7.41 (m, 4H). ¹³C NMR (100 MHz, DMSO-d₆): δ 55.4 (OCH₃), 56.4 (OCH₃), 56.8 (OCH₃), 107.8 (2× ArC–H), 110.3 (ArC–H), 110.8 (Pyrazole C=C), 112.9 (2× ArC–H), 115.6 (2× ArC–H), 117.9 (C=C), 118.1 (ArC–H), 119.5 (ArC–H), 122.2 (ArC–H), 124.6 (C=C), 129.6 (2× ArC–), 129.9 (C=C), 130.7 (C=C), 132.3 (Pyrazole C–N), 137.8 (ArC–N), 146.1 (2× ArC–OH), 146.8

(ArC–OCH₃), 148.0 (ArC–OCH₃), 148.9 (ArC–OCH₃), 154.1 (Pyrazole C=N). LCMS (ESI) m/z [M + 1]⁺ 471.54 Anal. calcd for C₂₈H₂₆N₂O₅ : C, 71.47; H, 5.57; N, 5.95; O, 17.00 Found : C, 71.49; H, 5.60; N, 5.97; O, 17.02.

Bioavailability studies

Compound preparation and ADME Prediction

QikProp, the prediction program used to calculate ADME properties. Compounds were drawn using Maestro 2D sketcher, each structure was launched in Ligprep for energy minimization using the OPLS force field 2005 and geometrically optimized. Lipinski's values/ADME prediction was executed by using QikProp v3.3. Qikprop modules provide the ranges of molecular predicting properties for comparing the properties of a particular molecule with those of 95 % of known drugs (Lipinski et al., 2001).

Biological studies

Three different cancer cell lines, MCF-7, HeLa, and K562 cells, were selected for the preliminary anticancer screening of curcumin pyrazole derivatives (**3a–3e**). MTT assay was employed to assess the growth inhibitory potential of the curcumin analogs (Sharath Kumar et al., 2015) with few modifications. Further, analysis of progression of cell cycle and mitochondrial membrane potential assay were performed by flow cytometry to confirm the mechanism of induction of cell death in compound **3b** treated K562 cells (Vinaya et al., 2011; Sharath Kumar et al., 2014).

Cell lines and culture

HeLa (Human cervical cancer cell line), MCF-7 (Human breast cancer cell line), K562 (human myelogenous leukemia cell line), and HEK293T (Human embryonic kidney cell line) cells were purchased from National centre for cell science, Pune, India. Cells were grown in RPMI 1640 supplemented with 10 % heat inactivated fetal bovine serum, 100 U/ml of penicillin and 100 µg of streptomycin/ml and incubated at 37 °C in a humidified atmosphere with 5 % CO₂.

MTT assay

The cytotoxic effects of the synthesized compounds against the cervical carcinoma, breast carcinoma, and leukemic cells (5 × 10⁵ cells) were assessed using 3-(4,5-dimethyl-2-yl)-2,5-diphenyl tetrazolium bromide (MTT) assay. Embryonic kidney cell lines were utilized to assess the growth suppressive effects of the potent cytotoxic compound in the series by MTT assay. The test compounds

were dissolved in DMSO and treated with different concentrations of synthesized compounds **3a–3e** (10, 20, and 40 μ M, respectively). Cells in the control wells received the same volume of medium containing DMSO. After 48 and 72 h treatment cells were harvested and incubated with MTT (0.5 μ g/ml) for 4 h at 37 °C in 96-well plate. The blue MTT formazan precipitate formed in the viable cells is solubilized by the addition of 70 μ l DMSO. The suspension is placed in microvibrator for 5 min and absorbance was measured at 540 nm using multimode reader (Varioskan Flash Multimode, Thermo scientific, USA). The experiment was performed in triplicate and repeated at least for three times.

Cell cycle analysis using fluorescent activated cell sorter analysis

K562 cells were seeded in 24-well plate at 0.75×10^5 cells/ml of complete growth culture media, incubated for 24 h. After incubation, the cells were treated with different concentrations of compound **3b** (10, 20, and 40 μ M). After 48 h the cells were harvested, washed with 1 \times PBS, and then fixed in 70 % ethanol at 4 °C overnight. Before acquiring to flow cytometry, cells are washed with 1 \times PBS and resuspended in 300 μ l 1 \times PBS. RNase (50 μ g/ml) (Sigma Aldrich, USA) treatment was given and finally stained with propidium iodide (Sigma Aldrich, USA) and subjected to flow cytometry (Beckman Coulter, USA) using CellQuest Pro Software, excitation 488 nm laser, and emission at 560/670 nm. DNA content of 10,000 cells was recorded per sample and histograms were analyzed by Flowing Software (version 2.5).

Mitochondrial membrane potential assay

JC-1 (5,5'-6,6'-tetrachloro-1,1'-tetraethyl benzimidazolyl carbocyanine iodide (Calbiochem, USA), a sensitive dye which gives an appropriate measure of the changes in mitochondrial transmembrane potential ($\Delta\psi$ m) was employed. K562 cells were treated with compound **3b** (10, 20, and 40 μ M, respectively). Cells were harvested after 48 h and incubated with JC-1 (0.5 μ M) at 37 °C for 30 min. Further, cells were washed with 1 \times PBS and the cells were subjected to flow cytometric analysis using CellQuest Pro Software, an excitation at 488 nm laser, and emission at 530/630 and 580/610 nm. Total 10,000 cells were acquired per sample. Results were analyzed in WinMDI 2.9 software and data were presented.

Statistical analysis

The analysis was performed by using a GraphPad Software Prism 5.1. All the values are expressed as mean \pm SEM for

samples and are statistically analyzed. One-way ANOVA followed by Dunnett test was used; in each case experimental samples were compared with control and significance was determined. p -value ≤ 0.05 was considered as statistically significant.

Acknowledgments The authors express sincere gratitude to Dr. S Nagendra, Managing Director and Chief executive officer, Scintilla BIO-MARC pvt. Ltd, Bangalore, India for providing technical assistance regarding cell culture facilities for the work.

Compliance with ethical standards

Conflict of interest The authors declare that they have no conflict of interest.

References

- Aggarwal BB, Kumar A, Bharti AC (2003) Anticancer potential of curcumin: preclinical and clinical studies. *Anticancer Res* 23:363–398
- Aggarwal BB, Sundaram C, Malani N, Ichikawa H (2007) Curcumin: the Indian solid gold. *Adv Exp Med Biol* 595:1–75
- Aggarwal S, Ichikawa H, Takada Y, Sandur SK, Shidhodia S, Aggarwal BB (2006) Curcumin (diferuloylmethane) down-regulates expression of cell proliferation and antiapoptotic and metastatic gene products through suppression of I-kappa B-alpha kinase and Akt activation. *Mol Pharmacol* 69:195–206
- Anand P, Kunnumakkara AB, Newman RA, Aggarwal BB (2007) Bioavailability of curcumin: Problems and promises. *Mol Pharm* 4:807–818
- Anand P, Sundaram C, Jhurani S, Kunnumakkara AB, Aggarwal BB (2008) Curcumin and cancer: an “old-age” disease with an “age-old” solution. *Cancer Lett* 267:133–164
- Anand P, Thomas SG, Kunnumakkara AB, Sundaram C, Harikumar KB, Sung B, Tharakan ST, Misra K, Priyadarsini IK, Rajasekharan KN, Aggarwal BB (2008) Biological activities of curcumin and its analogues (congeners) made by man and mother nature. *Biochem Pharmacol* 76:1590–1611
- Balbi A, Anzaldi M, Maccio C et al (2011) Synthesis and biological evaluation of novel pyrazole derivatives with anticancer activity. *Eur J Med Chem* 46(5293):309
- Chandru H, Sharada AC, Ananda kumar CS, Rangappa KS (2008) Antiangiogenic and growth inhibitory effects of synthetic novel 1, 5-diphenyl-1,4 pentadiene-3-one-3-yl-ethanone pyridine curcumin analogues on ehrlich ascites tumor in vivo. *Med Chem Res* 17:515–529
- Chandru H, Sharada AC, Bettadaiah BK, Ananda kumar CS, Rangappa KS, Sunila, Jayashree K (2007) In vivo growth inhibitory and anti-angiogenic effects of synthetic novel dienone cyclopropano curcumin analogs on mouse ehrlich ascites tumor. *Bioorg Med Chem* 15:7696–7703
- Chandru H, Sharada AC (2007) Antiangiogenic effects of synthetic analogs of curcumin in vivo. *Afr J Biomed Res* 10:241–248
- Davis R, Das U, Mackay H, Brown T, Mooberry SL, Dimmock JR, Lee M, Pati H (2008) Syntheses and cytotoxic properties of the curcumin analogs 2,6-Bis(benzylidene)-4-phenylcyclohexanones. *Arch Pharm Chem Life Sci* 341:440–445
- Devi PU, Solomon FE, Sharada AC (1999) Plumbagin, a plant naphthoquinone with antitumor and radiomodifying properties. *Pharma Biol* 37:231–236

- Duvoix A, Blasius R, Delhalle S, Schnekenburger M, Morceau F, Henry E et al (2005) Chemopreventive and therapeutic effects of curcumin. *Cancer Lett* 223:181–190
- Ferrari M, Fornasiero MC, Isetta AM (1990) MTT colorimetric assay for testing macrophage cytotoxic activity in-vitro. *J Immunol Methods* 131:165–172
- Fuchs JR, Pandit B, Bashin D, Etter JP, Regan N, Abdelhamid D, Li C, Lin J, Li PK (2009) Structure–activity relationship studies of curcumin analogues. *Bioorg Med Chem Lett* 19:2065–2069
- Fujii S, Okinaga T, Ariyoshi W, Takahashi O, Iwanaga K, Nishino N, Tominaga K, Nishihara T (2013) Mechanisms of G1 cell cycle arrest and apoptosis in myeloma cells induced by hybrid-compound histone deacetylase inhibitor. *Biochem Biophys Res Commun* 434:413–420
- Gopal PK, Paul M, Paul S (2014) Curcumin induces caspase mediated apoptosis in JURKAT cells by disrupting the redox balance. *Asian Pac J Cancer Prev* 15:93–100
- Koca I, Ozgur A, Coskun KA, Tutar Y (2013) Synthesis and anticancer activity of acyl thioureas bearing pyrazole moiety. *Bio Med Chem* 21:3859–3865
- Kumar D, Mishra PK, Anand AVK, Agrawal PK, Mohapatra R (2012) Isolation, synthesis and pharmacological evaluation of some novel curcumin derivatives as anticancer agents. *J Med Plants Res* 6:2880–2884
- Lee DS, Lee MK, Kim JH (2009) Curcumin induces cell cycle arrest and apoptosis in human osteosarcoma (HOS) cells. *Anticancer Res* 29:5039–5044
- Lipinski CA, Lombardo F, Dominy BW, Feeney PJ (2001) Experimental and computational approaches to estimate solubility and permeability in drug discovery and development settings. *Adv Drug Deliv Rev* 46:3–26
- Liu E, Wu J, Cao W, Zhang J, Liu W, Jiang X, Zhang X (2007) Curcumin induces G2/M cell cycle arrest in a p53-dependent manner and upregulates ING4 expression in human glioma. *J neuro oncol* 85:263–270
- Liu T, Tan Z, Jiang L, Gu JF, Wu XS, Cao Y, Li M, Wu K, Liu Y (2013) Curcumin induces apoptosis in gallbladder carcinoma cell line GBC-SD cells. *Cancer cell Int* 13:64–72
- Ly JD, Grubb R, Lawen A (2003) The mitochondrial membrane potential ($\Delta\psi_m$) in apoptosis; an update. *Apoptosis* 8:115–128
- Mayadevi M, Sherin DR, Keerthi VS, Rajashekaran KN, Omkumar RV (2012) Curcumin is an inhibitor of calcium/calmodulin dependent protein kinase II. *Bioorg Med Chem* 20:6040–6047
- Mishra S, Karmodiya K, Surolia N, Surolia A (2008) Synthesis and exploration of novel curcumin analogues as anti-malarial agents. *Bioorg Med Chem* 16:2894–2902
- Newman DJ, Cragg GM, Snadder KM (2003) Natural products as sources of new drugs over the period 1981–2002. *J Nat Prod* 66:1022–1037
- Ohuri H, Yamakoshi H, Tomizawa M, Shibuya M, Kakudo Y, Takahashi A, Takahashi S, Kato S, Suzuki T, Ishioka C, Iwabuchi Y, Shibata H (2006) Synthesis and biological analysis of new curcumin analogues bearing an enhanced potential for the medicinal treatment of cancer. *Mol Cancer Ther* 5:2563–2571
- Pan MH, Huang TM, Lin J (1999) Biotransformation of curcumin through reduction and glucuronidation in mice. *Drug Metab Dispos* 27:486–494
- Pramod KS, Praveen KS, Gupta SK, Thavaselvam D, Agarwal DD (2012) Synthesis and evaluation of antimicrobial activity of 4H-pyrimido[2,1-b]benzothiazole, pyrazole and benzylidene derivatives of curcumin. *Eur J Med Chem* 54:366–378
- Rocha AB, Lopes RM, Schwartzmann G (2001) Natural products in anticancer therapy. *Curr Opin Pharmacol* 1:364–369
- Senft C, Polacin M, Priester M, Seifert V, Kogel D, Weissenberger J (2010) The non toxic natural compound Curcumin exerts antiproliferative, anti-migratory and anti-invasive properties against malignant gliomas. *BMC Cancer* 10:491–498
- Shamroukh AH, Rashad AE, Abdel-Megeid RE, Ali HS, Ali MM (2014) Some pyrazole and pyrazolo(3,4-d)pyrimidine derivatives: Synthesis and anticancer evaluation. *Arch Pharm Chem Life Sciences* 347:559–565
- Sharath Kumar KS, Hanumappa A, Hegde M, Narasimhamurthy KH, Raghavan SC, Rangappa KS (2014) Synthesis and antiproliferative effect of novel 4-thiazolidinone-pyridine- and piperazine-based conjugates on human leukemic cells. *Eur J Med Chem* 81:341–349
- Sharath Kumar KS, Hanumappa A, Vetrivel M, Hegde M, Girish YR, Byregowda TR, Rao S, Raghavan SC, Rangappa KS (2015) Antiproliferative and tumor inhibitory studies of 2,3 disubstituted 4-thiazolidinone derivatives. *Bioorg Med Chem Lett* 25:3616–3620
- Steward WP, Brown K (2013) Cancer chemoprevention: a rapidly evolving field. *Br J Cancer* 109:1–7
- Thangapazham RL, Sharma A, Maheshwari RK (2006) Multiple molecular targets in cancer chemoprevention by curcumin. *AAPS J* 8:443–449
- Tsao AS, Kim ES, Hong WK (2004) Chemoprevention of cancer. *Cancer J Clin* 54:150–180
- Vinaya K, Kavitha CV, Chandrappa S, Prasanna DS, Raghavan SC, Rangappa KS (2011) Synthesis and antileukemic activity of novel 4-(3-(piperidin-4-yl) propyl)piperidine derivatives. *Chem Biol Drug Des* 78:622–630
- Wang J, Qi L, Zheng S, Wu T (2013) Curcumin induces apoptosis through the mitochondria-mediated apoptotic pathway in HT-29 cells. *J Zhejiang Univ Sci B* 10:93–102
- Wang YJ, Pan MH, Cheng AL, Lin LI, Ho YS, Hsieh CY, Lin JK (1997) Stability of curcumin in buffer solutions and characterization of its degradation products. *J Pharm Biomed Anal* 15:1867–1876
- Yin HT, Tian QZ, Guan L, Zhou Y, Huang XE, Zhang H (2013) In vitro and in vivo evaluation of the antitumor efficiency of resveratrol against lung cancer. *Asian Pac J Cancer Prev* 14:1703–1706
- Youssef KM, Magda A, El-Sherbeny (2005) Synthesis and antitumor activity of some curcumin analogs. *Arch Pharm Chem Life Sci* 338:181–189